Satellite-Based Approaches in the Detection and Monitoring of Selected Hydrometeorological Disasters

Satellite-based approaches in the detection and monitoring of selected hydrometeorological disasters

Paola Mazzoglio[1, *], Andrea Ajmar[2], Guy J.P. Schumann[3,4], Simone Balbo[5], Piero Boccardo[6], Francesca Perez[7], Enrico Borgogno-Mondino[8]

[1] Department of Environment, Land and Infrastructure Engineering, Politecnico di Torino, 10129 Turin, Italy. paola.mazzoglio@polito.it

[2] Interuniversity Department of Regional and Urban Studies and Planning, Politecnico di Torino, 10125 Torino, Italy. andrea.ajmar@polito.it

[3] School of Geographical Sciences, University of Bristol, Bristol, BS81SS UK. gjpschumann@gmail.com

[4] Dartmouth Flood Observatory (DFO), University of Colorado Boulder, Boulder, CO, USA.

[5] ITHACA - Information Technology for Humanitarian Assistance, Cooperation and Action, 10138 Torino, Italy. simone.balbo@ithaca.polito.it

[6] Interuniversity Department of Regional and Urban Studies and Planning, Politecnico di Torino, 10125 Torino, Italy. piero.boccardo@polito.it

[7] ITHACA - Information Technology for Humanitarian Assistance, Cooperation and Action, 10138 Torino, Italy. francesca.perez@ithaca.polito.it

[8] Department of Agricultural, Forest and Food Sciences, Università degli Studi di Torino, 10095 Grugliasco, Italy. enrico.borgogno@unito.it

[*] Corresponding author.

Abstract

Currently, Earth Observation (EO) satellite systems are playing an increasingly important role in the provision of a wide range of information, especially in data-scarce regions. This role becomes extremely relevant when a disaster is ongoing, and direct access to the affected area is difficult. In a perspective of disaster preparedness, rainfall measurements provided by satellites can enable decision-makers to take urgent measures in the pre-event phase and can be used as input for early warning systems. Data acquired from satellite missions are used for a set of different tools

developed to map flood extent, while several satellite-based emergency mapping mechanisms provide timely post-event information by taking advantage of observations provided by satellites (including commercial platforms providing images at very high geometric resolution). This chapter provides an overview of the state of the art of remote sensing techniques and tools for the identification and monitoring of hydro-meteorological disasters, with an application on the area affected by Cyclones Idai and Kenneth in 2019. Analysis of vegetation dynamics derived from time-series of multispectral imagery is used to estimate a variety of damages, such as the detection of main crop/vegetation affected areas, identification of critical conditions in vegetation health/productivity and land cover change mapping.

Keywords

cyclone; flood; hurricane; rainfall; remote sensing; satellite

1. INTRODUCTION

In recent years, hurricanes and tropical storms have been particularly devastating globally, with rainfall and inundation footprints far exceeding records and national response capabilities. On a global basis, severe floods are frequent and cause massive damage to societies and economic systems, jeopardizing infrastructure, transportation and communication networks and reducing crop yields. In addition to the high number of people killed or displaced from their homes, floods affect human health for long periods. According to the Emergency Events Database (EMDAT), flood events are the natural disasters that have affected the greatest number of people in the 21st century. Single disastrous flood events can affect and displace many hundreds of thousands of people, cause several hundreds of deaths, and cost billions of USD in damages. The 2019 South-West Indian Ocean cyclone season, with Cyclones Idai in March and Kenneth in April and numerous others, affected large areas in Mozambique and neighboring countries, devastated entire nations, and complete recovery from these disasters will most likely be impossible for most people in these regions (Schumann 2019). Considering the high vulnerability of people that live in that area, a detailed study is necessary to deeply investigate both the formation and the motion of tropical cyclones and heavy rainfall events in order to significantly reduce the number of people affected by water-related disasters. This objective is achievable through the integration of climate change measures into national strategies and the development of tools for disaster identification and monitoring.

Since high-impact large-scale events often cover an area beyond traditional regional monitoring operation, remote sensing presents an attractive approach (Schumann et al. 2018). Earth Observation (EO) could provide valuable information across various spatial and temporal scales, especially in data-scarce areas. Significant progress has been achieved in the field of EO in recent

years due to a continuous massive effort made by space agencies, scientists and many others alike. The proliferation of free satellite and geospatial data (Schumann and Domeneghetti 2016) necessitates action by the flood-expert community. In addition, the heterogeneous datasets already available require not only a profound understanding of the limitations and errors within the data and methods but also the development of more sophisticated algorithms for data processing. Robust frameworks for effective information management and transfer across networks are indeed of fundamental importance. Furthermore, the gap that currently exists between decision makers and scientists with regard to EO datasets requires the creation of a capacity-building community including scientists as well as stakeholders that can transform the proliferation of EO data into products that provide actionable information for better decision-making (Schumann and Domeneghetti 2016).

Many space agencies, including NASA and ESA, have increasingly been stepping up to these new challenges in flood monitoring and response by harnessing the full scope of their remote sensing and modelling resources during events, either through ongoing activities at research centers or through projects funding support. The overarching ultimate goal is to connect and demonstrate the integration of EO data and models into societal benefit areas with clear operational capabilities. Currently, significant efforts by experts in multiple domains are of fundamental importance for the creation of decision support tools or systems (DST or DSS) that effectively utilize remote sensing data. For instance, DSSs that collect relevant datasets, including EO and ground data and more recently also social media data (de Bruijn et al. 2019; Jongman et al. 2015), and bring it together in an interoperable service would significantly increase the return on investment for EO missions. A major challenge is to link the data and data service creators, working at a global scale, to the specific local end users. Increasingly, interoperable web services and related technologies are helping, as they allow for instant access to the latest available data and interoperability of various geospatial data systems.

2. LITERATURE REVIEW

In terms of flood disaster related activities, Schumann et al. (2018) summarize the state-of-the-art of existing efforts and systems operating under a public, open-access policy. All of these systems provide unique capabilities but, as noted, nearly all these systems are either voluntary or based on limited project funding, with the exception of the Disaster Charter and the Copernicus program (Schumann et al. 2018). In other words, none of those systems are sustained and managed in the long run without continuous funding and commitment. These EO-based systems range from collecting imagery, through to mapping and prediction of floods. There is however a desperate need to directly link what is being done at multiple organizations and agencies with the end-user community to support decision-making prior to and following a flood event.

2.1. Heavy rainfall monitoring tools

Recent advances in rainfall measurement allowed scientists to develop early warning systems like ITHACA Extreme Rainfall Detection System (ERDS), a service for the forecasting and monitoring of rainfall events at the global scale available through a WebGIS application (ERDS 2020). The Centre for Hydrometeorology and Remote Sensing (CHRS) at the University of California, Irvine (UCI), instead, recently developed a Data Portal for quick access of their satellite-based rainfall products (Nguyen et al. 2019). The portal also offers the opportunity to be redirected to iRain, a data visualization platform that provides near real-time information about accumulated rainfall based on the PERSIANN Dynamic Infrared-Rain rate model (PDIR; Nguyen et al. 2020). Moreover, iRain can identify and track extreme precipitation events globally, providing also a short report containing storm statistics. End-users can subscribe to intense rainfall alerts after having chosen a rainfall threshold and a location.

2.2. Flood identification tools

The Global Flood Observatory at the University of Colorado Boulder (CO, USA), known as the Dartmouth Flood Observatory or DFO, tracks, monitors and archives flood events globally since 1985 and makes data available in various formats including graphics, spreadsheets and GIS maps (DFO 2020a). This historic archiving of flood disasters represents crucial information for flood event analytics at global level, such as event dates, duration, geographic area, economic impact and number of lives lost. In addition, its open-access policy has recently enabled the development of young EO-based flood analytics businesses. The DFO also works in close collaboration with the Global Flood Partnership, which is a participating organization, to build the needed connections at the local level. By comparing, integrating and providing access to these complementary flood prediction, detection, measurement and mapping systems, the community provides end users with greatly improved flood information at the global scale.

The Global Flood Monitoring System (GFMS) is an experimental system developed by NASA and University of Maryland. TRMM Multi-satellite Precipitation Analysis (TMPA) and Global Precipitation Measurement (GPM) Integrated Multi-Satellite Retrievals for Global Precipitation Measurement (IMERG) data are used as input to a hydrological runoff and routing model characterized by a 1/8th degree lat/lon resolution and a 50°N – 50° S spatial coverage (Wu et al. 2014). Even at the relatively low resolution, the system allows the end-user to have timely information with a quasi-global spatial coverage and quick updates. Time series of water depth and streamflow with a 3-hours resolution were obtained at every grid point running the model retrospectively for 15 years. Flood detection is based on a flood threshold derived at grid cell level using surface water storage statistics like the 95th percentile and parameters related to basin characteristics. The system also issues short-term (4-5 days) flood forecasts based on numerical weather prediction (NWP) precipitation data.

Several international initiatives and organizations in which space agencies participate also provide other relevant services and geospatial data. This information "firehose" makes it difficult to coordinate all of the relevant systems during one single event while it becomes impossible with multiple simultaneous events. For instance, response activities to Hurricane Harvey (August 23 -

September 25, 2017) were still occurring as Hurricane Irma (September 4 - October 18, 2017) caused flood damage, and the same was true in Mozambique and neighboring countries during early 2019 in the case of Cyclones Idai and Kenneth. Although each of the response systems provides a "unique" capability, there is to date no global DSS that ingests all the data from existing systems and provides real-time "trusted" information about flood events.

2.3. Characteristics of the main Satellite Emergency Management mechanisms

As stated in the Emergency Mapping Guidelines developed by the International Working Group on Satellite-based Emergency Mapping (IWG-SEM), "Satellite-based Emergency Mapping (SEM) is defined as the creation of maps, geo-information products and spatial analyses dedicated to providing situational awareness for emergency management and immediate crisis information for response by means of extraction of reference (pre-event) and crisis (post-event) geographic information/data from satellite or aerial imagery" (IWG-SEM 2015). Data and products generated by SEM mechanisms are conceived to support civil protection authorities and international organizations in all phases of the emergency cycle (Voigt et al. 2016).

According to the UN-SPIDER Knowledge Portal (UN-SPIDER 2020), several SEM mechanisms are in place, to support disaster response operations through the provision of maps derived from satellite imagery:

- Copernicus Emergency Management Service (EMS) - Mapping component provides free of charge mapping service in cases of natural disasters, humanitarian crises and human-made emergency situations throughout the world (Copernicus EMS 2020). The products of the Mapping component generated in Rapid Mapping mode consist of standard mapping products delivered within hours or days from the activation in support of emergency management activities immediately following a disaster. The Risk & Recovery Mapping mode covers in particular activities dealing with prevention, preparedness, disaster risk reduction and recovery. The products delivered are based on the provision of satellite imagery from the Sentinel missions and the contributing missions that are made available through the Copernicus Space Component Data Access system (CSCDA). EMS can be triggered only by or through an Authorised User (AU). Authorised Users include National Focal Points in the EU Member States and countries participating in the Copernicus programme, as well as European Commission services and the European External Action Service (EEAS). Copernicus EMS is complemented by an early warning and monitoring component which includes systems for floods, droughts and forest fires;
- The International Charter on "Space and Major Disasters" is composed of space agencies and space system operators who work together to provide satellite imagery for disaster monitoring purposes (The International Charter Space and Major Disasters 2020). It is also supported by value-added providers, producing maps based on satellite data, and other partners providing data and services for specific regions of the world: Copernicus EMS and UNOSAT are within this group. The Charter can be activated at the request of AUs to support emergencies in their own country, as well as in a country with which they cooperate;

- UNITAR Operational Satellite Applications Programme (UNOSAT) provides satellite imagery analysis and capacity development to the UN system, UN member states, and its partners (UNOSAT 2020). UNOSAT benefits from a variety of sources for its satellite imagery: free and open-source, commercial vendors, the Charter (natural and technological disasters only), in-kind donations. UNOSAT can be activated by UN offices and agencies, government agencies, Red Cross and Red Crescent Movement, international and regional organizations and humanitarian Non-Governmental Organizations. The service is free of charge for UN sister agencies and humanitarian entities operating in line with UN policies;
- Sentinel Asia is a voluntary and best-efforts-basis initiative led by the Asia-Pacific Regional Space Agency Forum to share disaster information in near-real-time across the Asia-Pacific region (Sentinel Asia 2020);
- SERVIR, a joint venture between NASA and the U.S. Agency for International Development in Washington D.C., provides satellite-based Earth monitoring, imaging and mapping data, geospatial information, predictive models and science applications to help improve environmental decision-making among developing nations in eastern and southern Africa, the Hindu-Kush region of the Himalayas and the lower Mekong River Basin in Southeast Asia (NASA 2020);
- The Center for Satellite based Crisis Information (ZKI) is an institution of the German Aerospace Center (DLR) providing satellite-based analytics during disasters.

IWG-SEM aims to improve cooperation among SEM mechanisms, to better support emergency management and, in particular, its response phase. This objective is targeted through the implementation of mapping guidelines and the definition of standard formats to quickly exchange information on mapping activations among the different mechanisms (IWG-SEM 2014). Through the aggregation of GeoRSS feeds generated by every single mechanism, it is possible to obtain an overview of the different past and on-going activations.

2.4. Effects of flooding events on agriculture: monitoring damages by optical remote sensing

When trying to figure out the combined effects of floods on an agriculture-devoted area by optical remote sensing some issues have to be carefully taken into account. In this type of application, the expected role of optical data is not the detection of flooded areas, more effectively mapped by active remote sensing, but mapping and quantification of damages affecting crops/orchards. This task can be achieved: a) by comparing two single significant acquisitions preceding and following the event; b) looking at an entire time series (TS) of synthetic spectral indices (SI) covering a mid-long time period including the event. SI are mathematical aggregations of bands from EO data operating like proxies of time-varying features of vegetation (vigour, health, water content, etc). A widely used SI in vegetation monitoring is the Normalized Difference Vegetation Index (NDVI; Tucker 1979). Seasonal changes in NDVI TS proved to successfully track phenology (e.g. Pettorelli et al. 2005; Reed et al. 1994) as NDVI well correlates to vegetation productivity (Bai et al. 2008; Fensholt et al. 2006; Running et al. 2004) being mainly responsive to canopy chlorophyll content.

3. MATERIAL AND METHODS

3.1. Heavy rainfall identification

Two different analyses are currently implemented in ERDS. The first one is a near real-time rainfall monitoring based on GPM IMERG Early run data, a global (90°N – 90°S) rainfall measurement retrieved from satellite characterized by a 0.1° spatial resolution and a 30 minutes temporal resolution, available with a 4 hours latency (Huffman et al. 2019). The second analysis is based on a weather prediction model called Global Forecast System (GFS). GFS model runs 4 times a day, providing data characterized by a global spatial coverage and a 0.25° spatial resolution. Heavy rainfall alerts are issued after having performed a comparison between accumulated rainfall and rainfall threshold (Mazzoglio et al. 2019). Threshold values are data-dependent (threshold values applied to GPM data are different to GFS ones) and time-dependent (threshold values increase as the aggregation interval increases).

3.2. Flood identification

Since 2011, the DFO has collaborated with the NASA Goddard Space Flight Center (GSFC) and other US and international organization in distributing near real-time flood maps from satellite imagery, primarily from Moderate Resolution Spectroradiometer (MODIS) onboard NASA's Aqua and Terra satellites (Brakenridge and Anderson 2006; Schumann et al. 2018), and also related EO data. The DFO also hosts a database of virtual stations of discharge records from 1998 until present based on an integration of microwave radiometry measurements and global hydrological modelling. The hydrological model (Water Balance Model, WBM; Fekete et al. 2002) is used for calibrating the microwave signal change (due to changes in surface water area occupying a pixel) to discharge. Specifically, these "River and Reservoir Watch" virtual stations (DFO 2020b) gauge the state of potential large river flooding daily based on changes in the brightness temperature of the passive microwave signal onboard the AMSR-E, TRMM, AMSR-2 and GPM sensors (Brakenridge et al. 2012).

More recently, the DFO has implemented an open geospatial service protocol. A Web Map Service (WMS) has been set up through which GIS clients can seamlessly ingest the latest up-to-date flood related products (Figure 1). The developed DSS for global flood information now includes an online GIS visualization interface built on a WMS that leverages existing systems and interoperability tools and standards (DFO 2020c): the idea is to ensure that systems and tools are not duplicated but leveraged and expanded. The online DSS has been complemented with a free mobile application ("DFO Floods") available on Android and Apple OS, which has the same functionalities and in addition allows the user to link in other free interoperable data services as well as offering offline capabilities by downloading map layers directly onto the mobile device. With these recent developments, decision-makers are able to pull data and products from the DSS at low bandwidth and latency, and also directly request from the DFO tailored information layers as needed for their operations, which was the case for instance for the Harvey event in 2017. Other relevant information is made available alongside remotely sensed flood data, such as output layers from ECMWF forecasts and from global flood hazard models (Dottori et al. 2016).

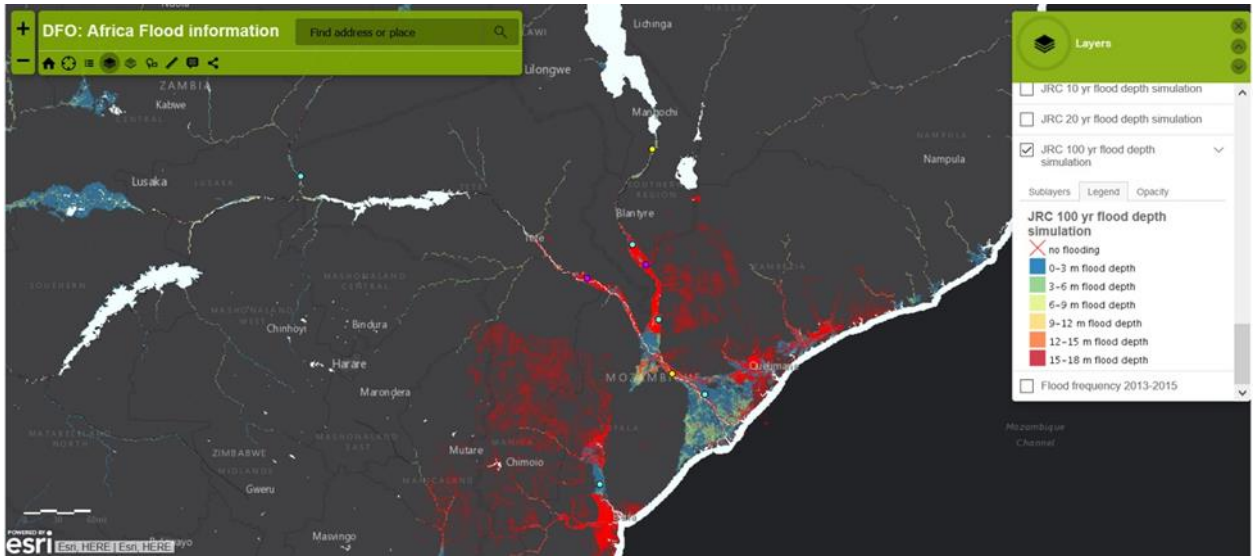

Figure 1. DFO's WMS. Map overlaying an open map layer shows in red flooding mapped during the events in Mozambique and neighboring countries in early 2019 up to March. Regular waters are depicted in light gray. River and Reservoir Watch stations are represented in colors relating to severity of flow. Flood depths from the JRC global flood hazard model of the 100-years return period flows are also shown.

3.3. Satellite Emergency Mapping mechanisms response to Cyclones Idai and Kenneth

Tropical Cyclone Idai made landfall as a Category 2 storm during the night of 14 March 2019 near the city of Beira, a city with approximately 500,000 inhabitants in Mozambique. Heavy rainfall, storm surges and strong winds caused significant damage to critical infrastructure and crops: it has been calculated that more than 100,000 homes were affected. Local authorities have reported 150 fatalities and more than 1,500 injured, and the National Institute for Disaster Management (INGC) estimated that 600,000 needed urgent assistance (Copernicus EMS 2019a).

Copernicus EMS, the Charter, UNITAR-UNOSAT and DLR-ZKI were all activated. In the framework of the Charter only, 320 satellite acquisitions have been performed, even if not all used because of limitations (e.g. cloud coverage) or almost overlapping characteristics (similar sensors, footprints and acquisition date/times). Figure 2 shows the footprints of satellite acquisitions. Radar images have generally a wider swath and larger overall coverage: they are intended to capture as far as possible the full extent of the flooded areas (delineation products). Earlier products have been generated mainly on this category of images, thanks to the all-weather capabilities of those sensors, capable of penetrating the residual cloud coverage. Optical images based analysis came in a second stage, with clearer skies, and was concentrated on the areas around Beira, to identify actual damages to infrastructures (grading products).

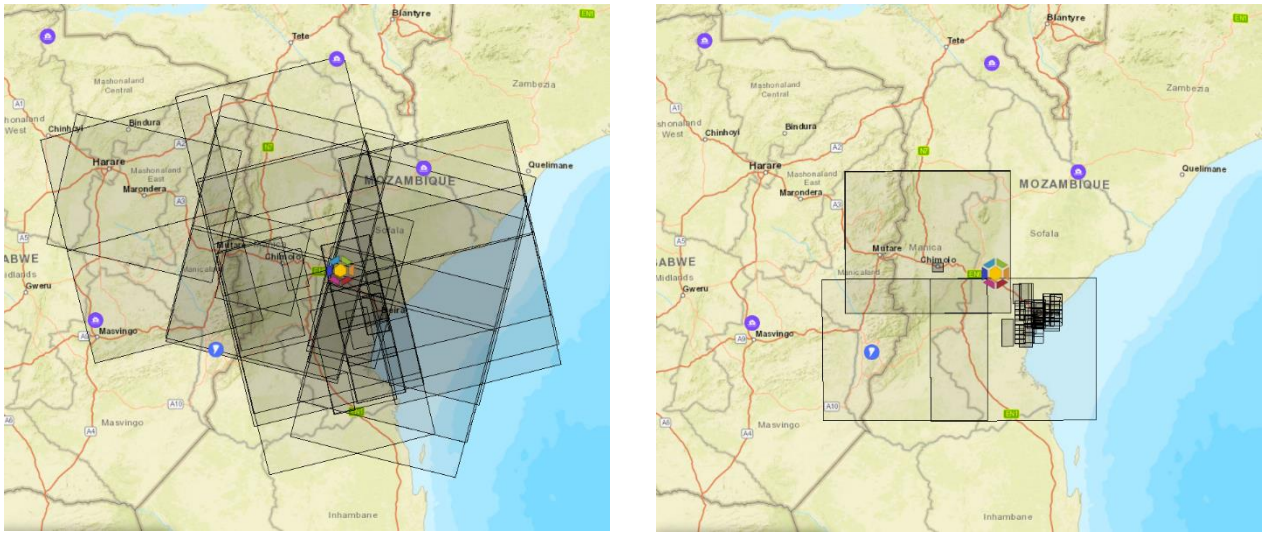

(a) (b)

Figure 2 - Satellite footprints of radar (a) and optical (b) images acquired in the framework of the Cyclone Idai activation (The International Charter Space and Major Disasters 2019a).

After passing through Comoros, Cyclone Kenneth made landfall on 25 April 2019 near the city of Pemba, in Mozambique: the area is sparsely populated and this is the main reason for the lower impact of this second cyclone in about a month hitting the same country. The Copernicus EMS Rapid Mapping module was activated on 26 April to provide Delineation and Grading Maps over several Areas of Interest along the coast of the Cabo Delgado province in Mozambique, and Grading Maps over the northern part of Comoros island. This was one of the first activation for which the product portfolio already included the "First Estimate Product" (FEP) which aims to provide a rough estimation of the disaster impacts within 2 hours from image reception and can be used to redefine Areas of Interest, that therefore are no more a hard constraint predefined by the user (Copernicus EMS 2019c).

3.4. Analysis of effects of flooding events on agriculture

Flooding is a very local phenomenon in nature. Consequently, when investigating damages, spatial information should be as much detailed as possible. In particular, in agriculture, the level of detail should be appropriate to the local average size of crop fields. Average crop field size can enormously vary around the world. Moreover, when vegetation is investigated, the temporal resolution of data is a very important feature to be taken into account. Among current EO satellite missions supplying free optical data having an appropriate temporal resolution, the Copernicus Sentinel-2 (S2) appears to be the most appropriate one. S2 records 13 spectral bands in the range 400-2500 nm, with a ground sampling distance (GSD) of 10 m, 20 m and 60 m (depending on the band), a 290 km swath and a nominal temporal resolution of 5 days. In particular, Level-2A product from Sentinel Data Hub, ortho-projected and bottom-of-atmosphere calibrated, well fits requirements of multi-temporal analysis. Currently, S2 data suffer from two great limitations for vegetation monitoring: a) the first observable growing season (GS) is the 2016 one and, therefore,

very short TS are available; b) its temporal resolution cannot be enough in those areas around the world where cloud cover is too frequent. Oppositely, Terra/Aqua MODIS data, having a temporal resolution of 1 day (or more) and a GSD up to 250 m, offer a good alternative. MODIS sensors have been operative since 2000 making freely available pre-processed products like the MOD13Q1/MYD13Q1 datasets containing composite maps of vegetation SI like NDVI and EVI (Enhanced Vegetation Index) with a time step of 16 days. Unfortunately, MODIS geometric resolution appears to be inadequate for a field-level investigation, moving the investigation from a local to a regional one. The ideal approach would be therefore a mixed one where MODIS-like data can be jointly used with S2-like ones.

Cloud cover analysis is mandatory to test if this approach could be reasonably successful. Analysis should drive to map occurrences of clouds, informing about local reliability of damage estimates. Comparison of time and position of cloud occurrences with growing calendars of main crops/orchards in the area can ensure about the feasibility of the analysis. Crop calendars define the period along the year when crops develop, reach maturation and are, finally, harvested. Knowledge about agronomic practices is desirable, as well.

When working with VI (vegetation index) TS, a typical workflow can be the following:

a) data selection/download from available archives and VI TS composition (stack);
b) data masking, regularization and smoothing aimed at selecting only vegetated pixels, removing "bad" observations from local VI temporal profiles, recovering profile continuity and minimizing residual noise;
c) TS modelling by detecting annual phenological cycles (e.g. Fast Fourier Transform analysis) that are singularly fitted by an interpolating model (e.g. asymmetric double logistic function; Hmimina et al. 2013);
d) accuracy assessment to test properness of model.

Output data are image stacks mapping modelled values of VI with a regular time step.

Phenological metrics (PM) represents synthetic parameters (Eklundh and Jönsson 2017) that characterize VI temporal profile. PM can be used to test if any significant variation has been induced onto crops phenology after a catastrophic event or as a consequence of climate change. Main PMs are:

- Start of Season (SOS), the Day of the Year (DOY) when GS starts;
- End of Season (EOS), the DOY when GS ends;
- Length of Season (LOS), the number of days separating EOS from SOS;
- MAX_VI, the maximum VI value within GS;
- MAX_DOY, the DOY when MAX_VI occurs;
- Season Amplitude (SA), the difference between the maximum and minimum VI value within GS;
- Rate of Increase, which is evaluated at the start of the season as the difference between the left 20% and 80% VI levels and the related difference in time;

- Rate of decrease, which is evaluated at the end of the season as the ratio of the difference between the right 20% and 80% VI levels and the related difference in time;
- Total productivity, the yearly integral of the fitted VI profile;
- Seasonal productivity or small integral (SMI), the integral calculated considering the fitted VI profile within SOS and EOS.

The availability of an updated map of crops is basic for a damage estimate. Often, available land use maps are not proper, being not updated and, frequently, supplied with a too high degree of class aggregation. Consequently, an up-to-date map of local crops has to be specifically generated for the period preceding the flooding event. Auxiliary information can come from official sources like FAO databases. Crop maps can be obtained by image classification according to two different approaches: one based on spectral signatures of crops in specific and limited times along the year; one based on a continuous monitoring of a spectral proxy (like VI) of the vegetative behavior (biomass production) of crops along with their GS. An example of differences in land cover mapping given by these approaches, obtained by a K-Means Iterative Minimum Distance unsupervised classification with a-posteriori class meaning interpretation, is shown in Figure 3.

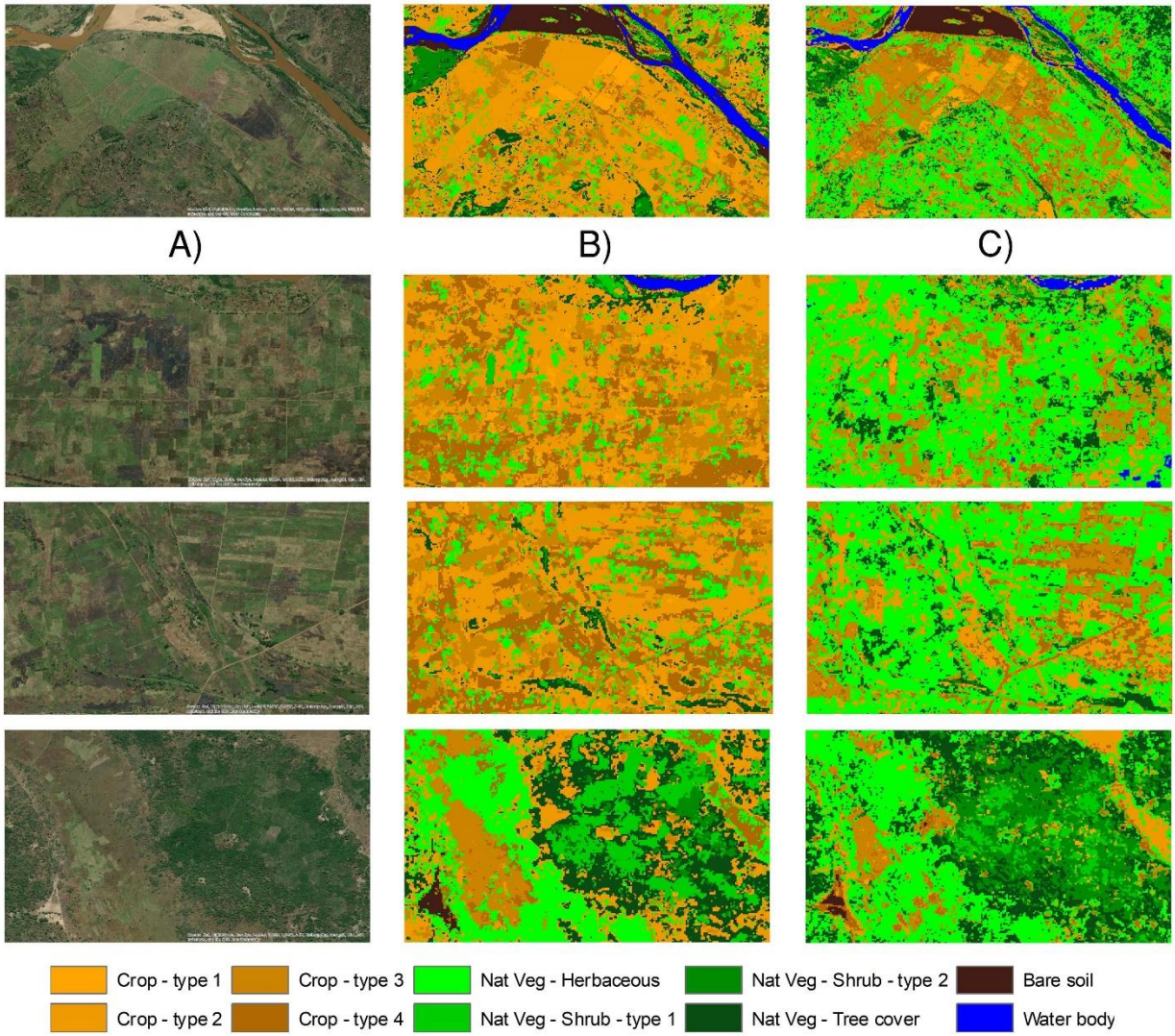

Figure 3. Examples of land cover maps obtained through unsupervised classification based on: b) NDVI monthly profile (August 2017 - November 2018) derived from Sentinel-2 imagery; c) VIS+NIR spectral signature extracted from Sentinel-2 multispectral monthly composite (July 2018). A high spatial resolution WorldView-3 image (DigitalGlobe Vivid mosaic; acquisition date 8/2/2018) is also reported for reference purposes (a). A K-Means Iterative Minimum Distance algorithm has been adopted, considering the following parameters: number of classes = 12; maximum number of iterations = 100 with change threshold value = 1%; standard deviation to use around the class mean = 0.05. Reported examples show that VI temporal profile-based classification better mapped crops, especially in those areas with high levels of land fragmentation and mixture of cultivated and natural vegetation classes. In fact, some crop types and natural vegetation classes (mainly herbaceous) present a low spectral separability if tested in a single monthly image (July, in this study).

4. RESULTS

4.1. Heavy rainfall identification: Cyclones Kenneth and Idai case study

The Extreme Rainfall Detection System (ERDS) provided timely alerts before Cyclones Idai and Kenneth landfall using GPM data as input (Table 1). Figure 4 shows the most affected areas, in terms of number of alerts provided by ERDS, along Idai track in the period between 5 and 24 March 2019, while Figure 5 shows the most affected area between 25 April and 1 May 2019 (during the progression of Kenneth).

AGGREGATION INTERVAL	CYCLONE IDAI DATE OF THE FIRST ALERT	CYCLONE KENNETH DATE OF THE FIRST ALERT
12 h	14/03/2019 10:30 UTC	25/04/2019 05:30 UTC
24 h	14/03/2019 11:00 UTC	25/04/2019 13:30 UTC
48 h	14/03/2019 11:00 UTC	25/04/2019 16:00 UTC
72 h	14/03/2019 14:00 UTC	25/04/2019 22:00 UTC
96 h	14/03/2019 16:00 UTC	26/04/2019 14:30 UTC

Table 1. Date and time of the first alert provided by ERDS using GPM data as input for the different aggregation intervals in the region where Idai made its second landfall on the coastal area between Beira and Quelimane (Mozambique) on 14 March 2019 at 23:30 UTC and in the region where Kenneth made its landfall on the coastal area near Pemba (Mozambique) on 25 April 2019 at around 16 UTC.

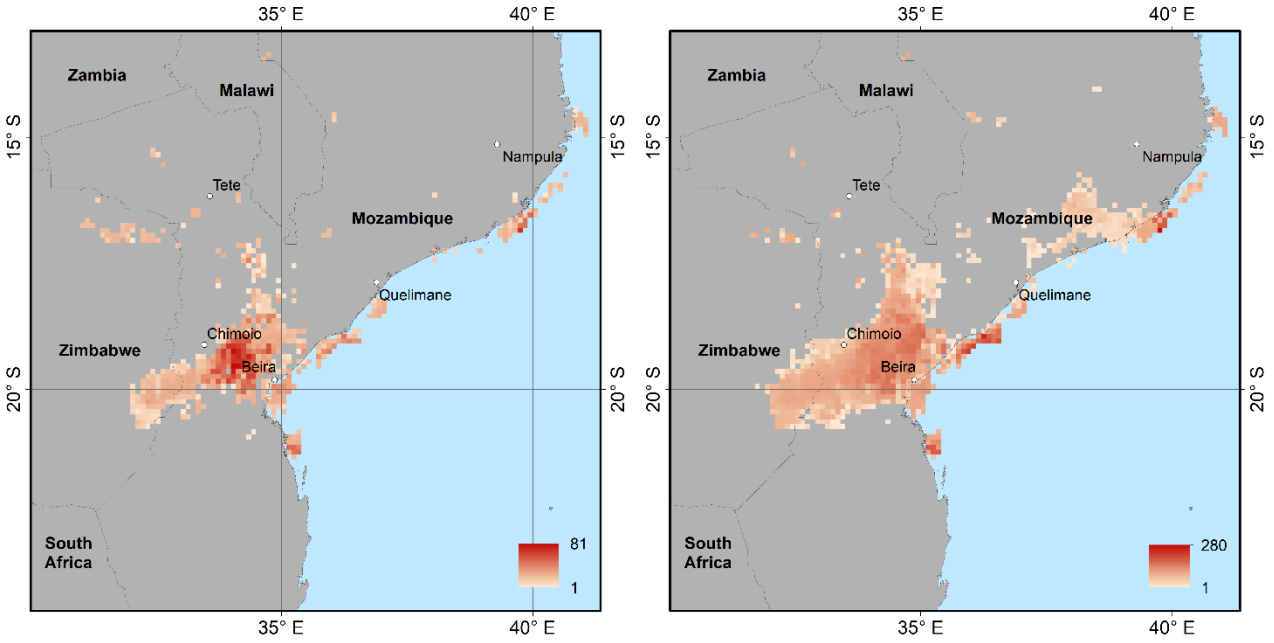

(a) (b)

Figure 4. Number of alerts provided by ERDS during the period between 5 and 24 March 2019 using GPM data as input and aggregation intervals equal to 12 hours (a) and 48 hours (b). Most of the alerts were issued in the area near Beira, where the combination of heavy rainfall and river overflow created an "inland ocean".

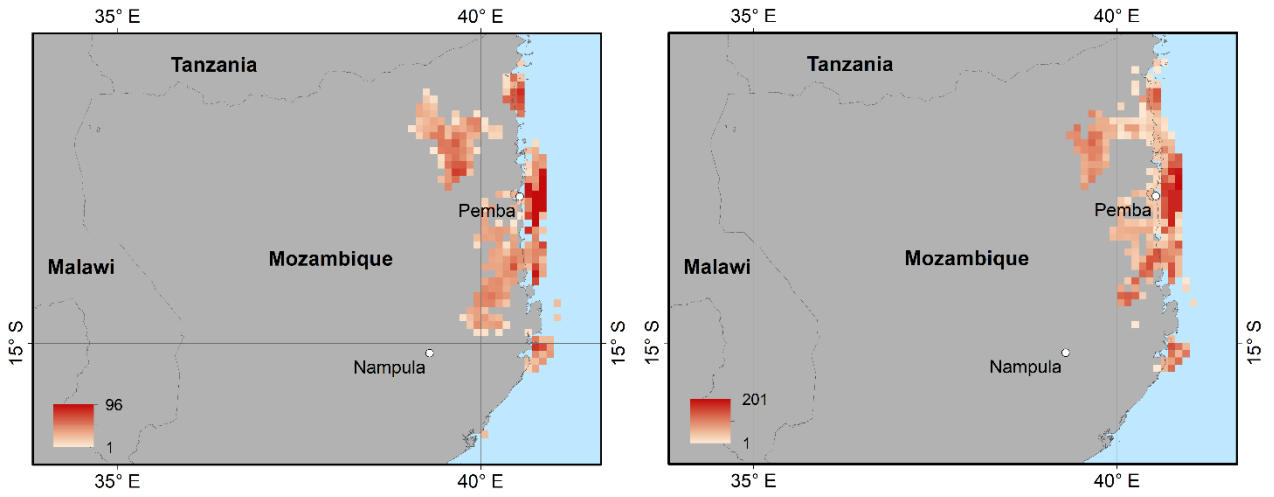

(a) (b)

Figure 5. Number of alerts provided by ERDS during the period between 25 April and 01 May 2019 using GPM data as input and aggregation intervals equal to 48 hours (a) and 96 hours (b).

4.2. Flood identification and damage assessment: Cyclones Kenneth and Idai case study

During high-impact flood disasters, the DFO maps flooding also from other satellites, such as the Landsat series and SAR satellite missions, and aggregates these products to several map formats that assist flood response teams through situational awareness across large scale coverages (Figure 6).

Figure 6. Mozambique: large scale flood mapping from various satellites, including MODIS, Landsat and ESA Sentinel-1. Blue areas: mean annual flood. Red areas: flooding in excess of mean annual flood. Light gray areas: maximum observed flooding, 1993 - Present. The colored dots are interactive and contain River and Reservoir Watch information.

Based on the available satellite images, in response to Cyclone Idai, Copernicus EMS generated 59 different products (9 reference, 36 delineation and 14 grading maps) covering three different countries: Malawi, Mozambique and Zimbabwe (Copernicus EMS 2019b). The Charter provided additional 20 maps and reports covering Mozambique (The International Charter Space and Major Disasters 2019c) and 10 in Zimbabwe (The International Charter Space and Major Disasters 2019d), thanks to the collaboration with UNOSAT, SEDEC/MDR, SERTIT, DLR/ZKI, UoL/NCEO, acting as value-added providers. Complementarities between mechanisms allowed to perform comprehensive impact analyses (ERCC – DG ECHO 2019b).

As far as Cyclone Kenneth concerns, Copernicus EMS generated 2 FEPs, 12 delineation and 35 grading map products in Mozambique and Comoros. The Charter has been activated over Mozambique only, providing 198 satellite acquisitions (The International Charter Space and Major Disasters 2019b), with similar characteristics to the one described and displayed in the case of Cyclone Idai. Two products were generated by Charter value-added providers. One map released by Copernicus EMS was based on imagery acquired in the framework of the Charter thereby acting also as a value-added provider.

Quantitatively estimating the impact of SEM in disaster risk management is a complex task, as many technological trends and operational organizations have to be considered and controlled. Demand for products and services generated by SEM initiatives and capacity building are generally rising worldwide and this can be considered as a qualitative indicator (Voigt et al. 2016). The added value of such products is widely recognised by "first responders" especially in case of major disasters, those requiring the mobilization of the international community: in most cases, they represent the only source of information on remote and inaccessible areas (Denis et al. 2016).

The full potential of these types of mechanisms will be exploited only through a better integration between services and responders. Related to Cyclone Idai, the Reliefweb repository alone contains 613 mapping and infographic products (as of 01/06/2020): up to the 22 March 2019, the day of the first damage assessment map released by Copernicus EMS, the three involved SEM mechanisms produced more than 20 maps having the water extents as main information. On 16 March 2019, WFP Logistic Cluster published the first of a series of maps highlighting access constraints (limitation affecting the usage of roads, ports and airports): those maps, released daily, never explicitly included the water extent layer released from the SEM mechanisms (WFP 2019). On 18 March 2019, MSF published a map reporting incidence reports for some districts. On the same day, the European Commission DG ECHO released the first map (ERCC – DG ECHO 2019a) combining meteorological information (cyclone path and rainfall accumulation), flooded areas and incident reports: following this last product, several organizations started producing new maps combining water extents with local assets. From this example it becomes evident that a better integration and exchange of information and data between services and responders would have allowed to streamline map production and to optimize resources, limiting the number of products reporting redundant information and increasing the timeliness in delivering ready-to-use products from the responder's perspective.

4.3. Damages to vegetation

A MODIS-based analysis was devoted to compare vegetation behaviour in terms of phenology during its growing season, before and after the flooding event with the aim of testing mid/long-term effects on agricultural production. S2 data were used to map existing crops at the moment of flood. The study area is presented in Figure 7.

In this work, cloud analysis involved 20 years of MODIS MOD13Q1 data, a composited product summarizing observations within a 16 days period. The MOD13Q1 quality layer (QL) reports information about the quality of each pixel by assigning a code that defines the eventual type of failure at that position, including cloud presence. It is, therefore, possible to generate a map of cloud occurrences and derive some spatially distributed information like total, mean, minimum and maximum occurrences along a year or in specific months (Figure 8).

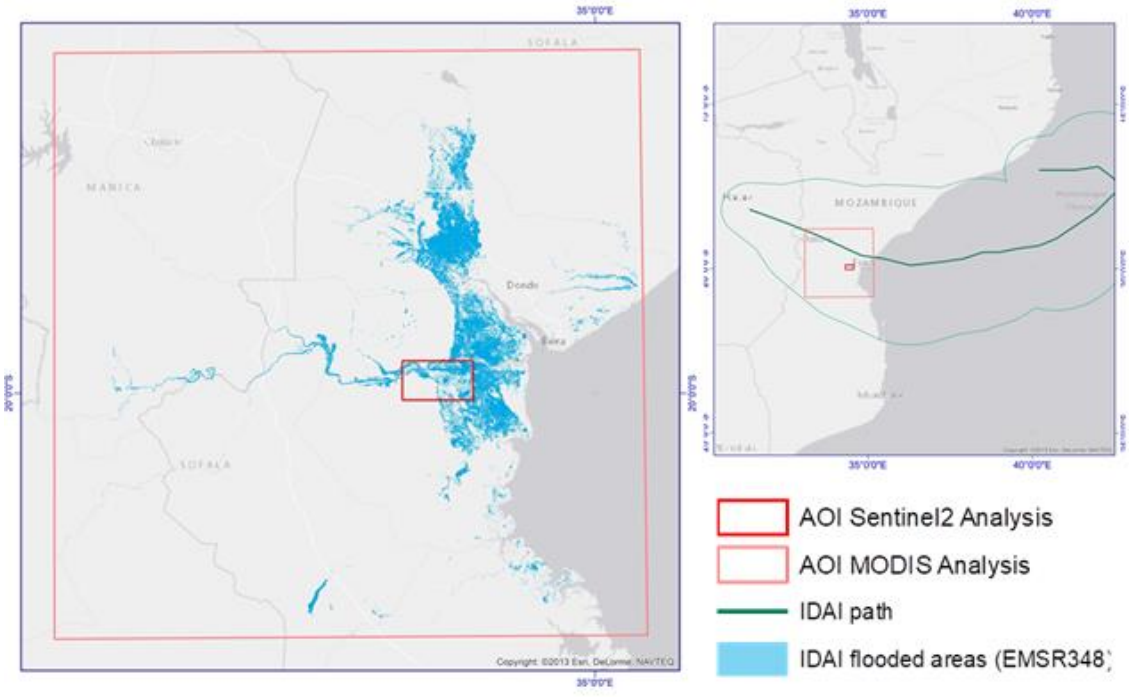

Figure 7. Study area. Regional investigation was achieved by MODIS data (pink rectangle) at a mid-term time scale (2000-2019). Local investigations, aimed at mapping crop types for economical estimation of damages, were carried out in the red squared area by S2 data in the period August 2017 - December 2018.

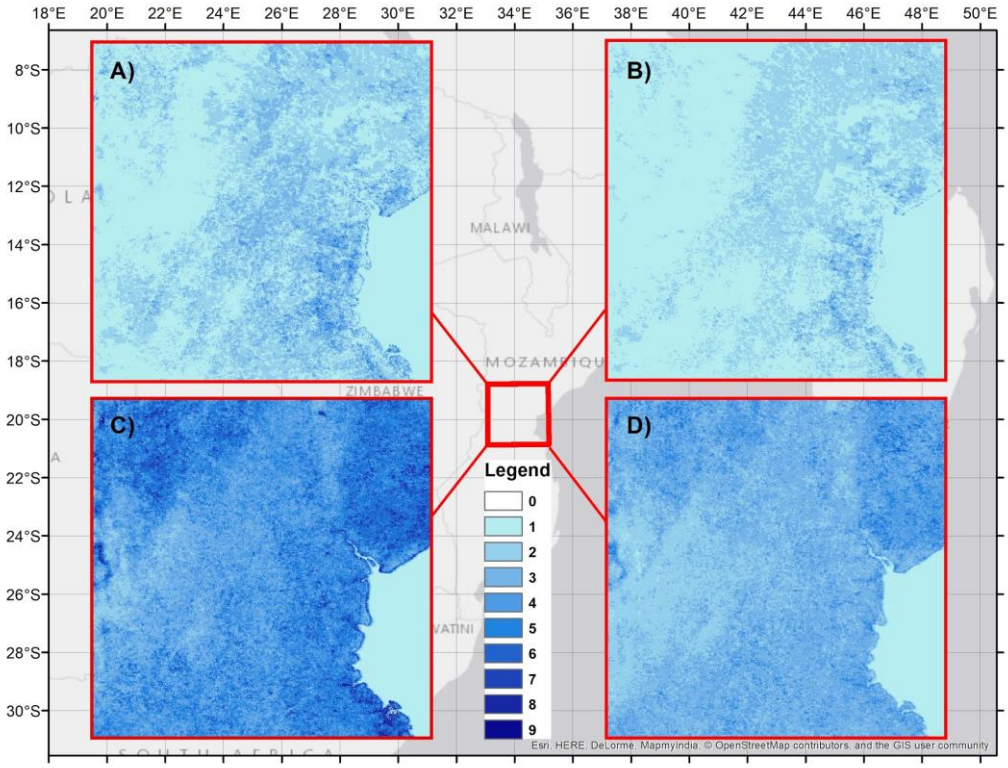

Figure 8. Cloud cover maps showing occurrences of clouds (derived from MOD13Q1 dataset) in the S2 investigated area. (A) = map of total number of "bad" occurrences in 2019; (B) = map of number of "bad" occurrences in February-May 2019; (C) = map of max number of "bad" occurrences in a year from 2000 to 2019; (D) = map of max number of "bad" occurrences in February-May from 2000 to 2019. The analysis showed a favorable situation (low cloud cover). Intra annual cloud cover shows, averagely in the area, a maximum value of 6 (out of about 23 yearly maps) occurrences of "bad" observations, with very local peaks of 6-9 occurrences. This value can be considered "not critical" for phenological analysis aimed at exploring the behaviour of crops along their growing season, especially if they do not occur sequentially. To test this issue a focus was done with reference to the period of the year when Cyclones Idai and Kenneth reached the area (March and April 2019). Four months (about 8 MOD13Q1 images) ranging from February-May 2019 where considered and the same period analyzed for all the years when MOD13Q1 data were available for (2000-2019). Averagely, a maximum of 4 "bad" observations (out of 12) was found with some local peaks of 6, confirming that a successful multitemporal analysis was possible in that period.

When trying to estimate damages affecting crops/orchard in a flooded area (Figure 9), two types of phenomena have to be taken into account: one concerning short term effects of flood,

basically affecting yearly yield and, consequently, limited in time; one concerning long-term effects on crops/orchard that need more GSs (years) to somehow recover.

A short-term damage estimate can be obtained intersecting a map of the flooded area, possibly coming from SEM mechanisms, with the previously mentioned map of crops. The area size of flooded crops multiplied by the average theoretical yield (kg/ha), obtainable from an official database (e.g. FAO), permits to estimate the annual loss of production and, consequently, convert it into an economical "georeferenced" loss. A long-term damage estimate (if present) can be differently investigated by multi-annual analysis based on long VI TS (MODIS scale). Comparison between crops GS of years preceding and following the flooding event permits to get information about this issue. In particular, PM comparison, often operated by anomaly (yearly PM value divided (or minus) the mean PM value along with TS) computation and mapping is one of the most adopted approaches. An example is reported in Figure 10.

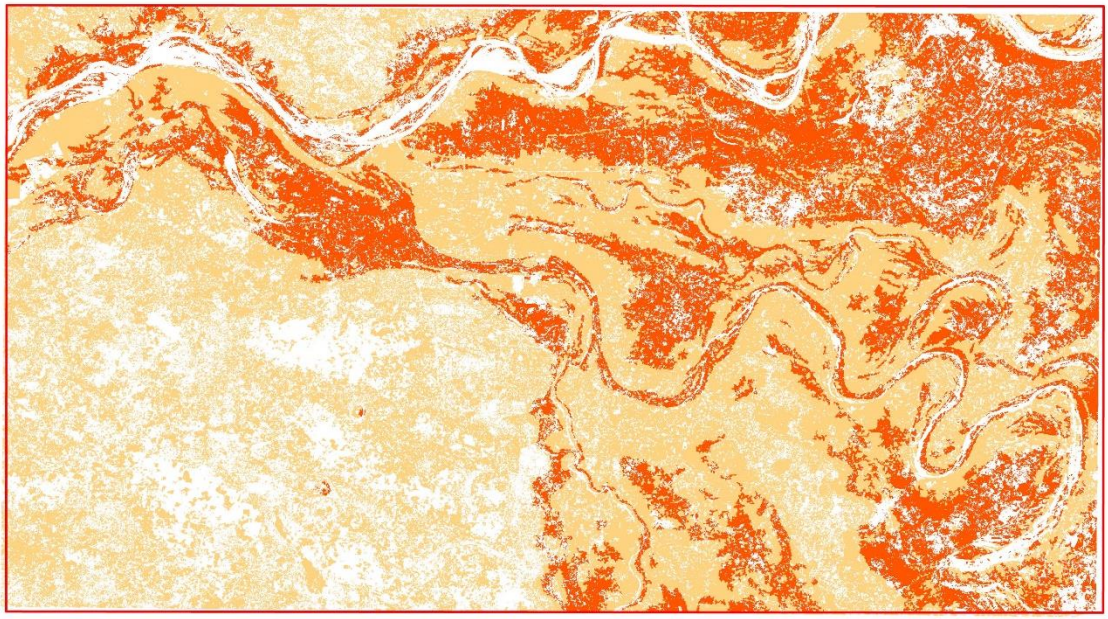

A)

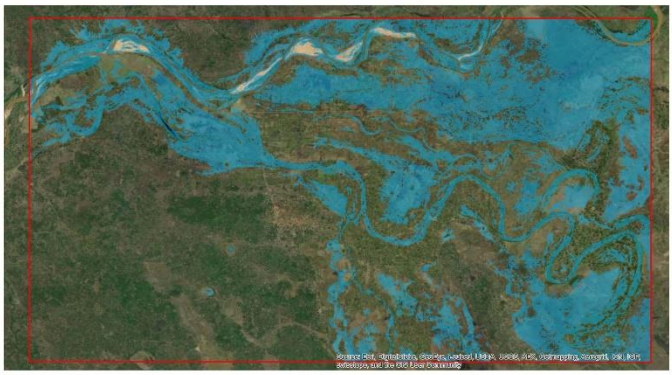

Study area - S2 image subset
Crop area
Flooded crop area
IDAI flooded areas (Copernicus EMS)

B)

	Crops in study area (S2 image subset) [ha]	Flooded crops in study area (S2 image subset) [ha]	Cereal Yield (2017) [kg /ha]	Seasonal (2017-2018) loss of production [t]
Crop type 1	1330,38	246,81		
Crop type 2	12715,65	3639,12		
Crop type 3	3498,50	1378,17		
Crop type 4	8703,24	4019,93		
TOTAL	**26247,77**	**9284,03**	**872**	**8095,67**

Figure 9. Map of flooded crop areas related to Cyclone Idai in 2019 (A). Cultivated areas have been mapped through NDVI temporal profile-based classification (2017-2018 growing season). Flooded area borders were defined in the frame of Copernicus EMSR384 specific operations (B). An estimate of related seasonal loss of production has been produced considering the most recent

value of cereal (generic) yield (kg/ha) in Mozambique, according to the World Bank collection of development indicators (World Bank 2020).

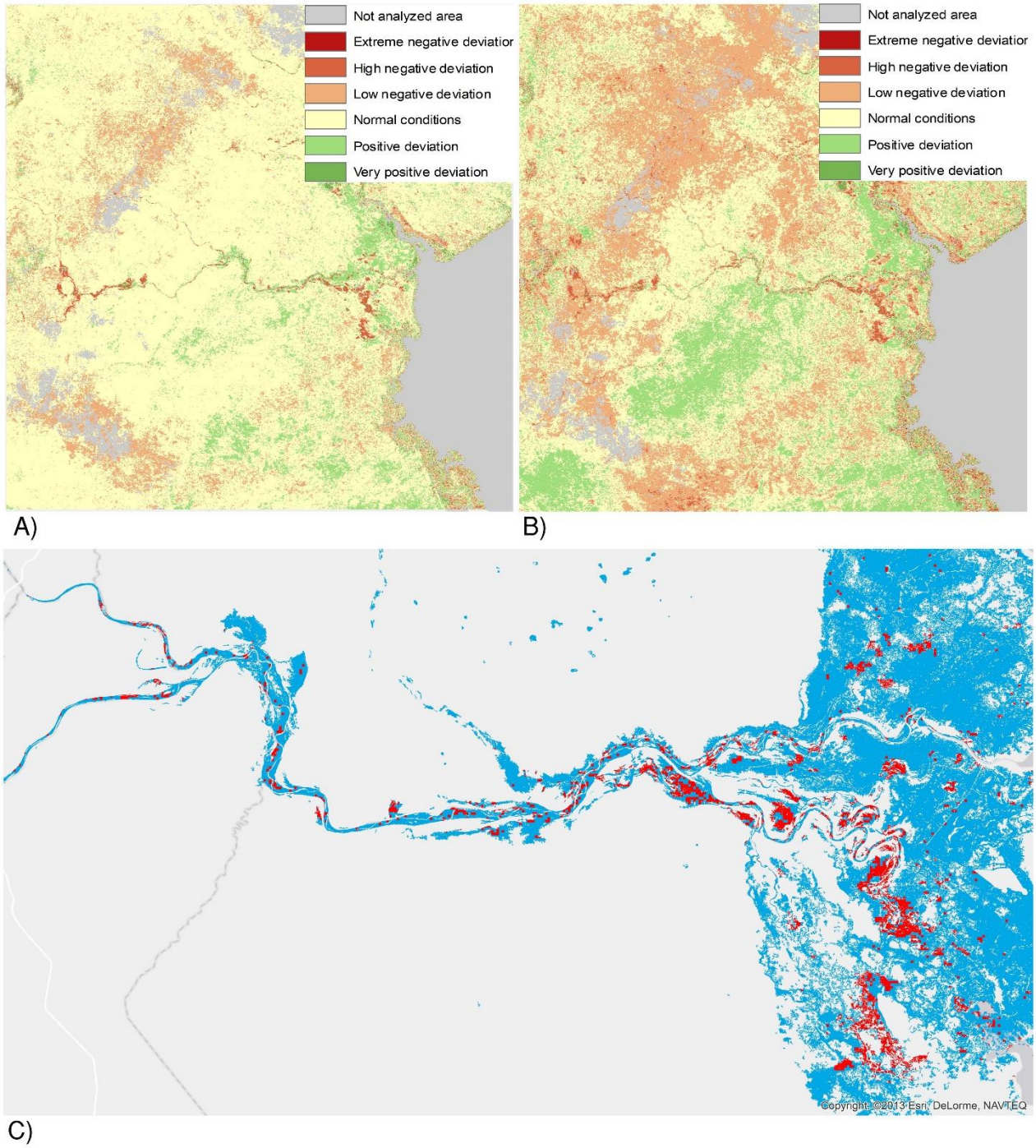

Figure 10. An example of anomaly maps of SMI (A) and LOS (B) computed with reference to the MOD13Q1 dataset for the 2018-2019 growing season, which was affected by the Cyclone Idai. Maps show the spatial distribution of percent deviations of selected phenological metric from to the historical average value (estimated from the 2000-2018 time-series). These maps, produced in near real-time or immediately after the examined growing season, can support the identification of critical areas where major damages to vegetation productivity are expected. Similar maps can be generated with reference to other significant PM for monitoring purposes and vegetation restoration evaluation. For the purpose of the examined case study, vegetated patches falling in the flooded areas (in blue in C) showing extreme negative LOS deviations were mapped (in red in C).

5. CONCLUSIONS

The chapter critically reviewed some of the most relevant EO-based techniques for near real-time identification and monitoring of heavy rainfall events. According to Target 11.5 of the 2030 Agenda for Sustainable Development, it is necessary to significantly reduce both the number of people affected by natural disasters and economic losses (UN General Assembly 2015). Remote sensing represents a viable solution for addressing this challenge, especially in areas without extensive monitoring networks. Even if the coarse spatial resolution affects the reliability of hydrological studies at the local scale, remote sensing products are able to provide accurate measurement for the identification of areas affected by extreme rainfall. The role of global sensing and modelling systems in addressing local disasters, however, requires clarification. Much orbital sensing provides global or near-global geographic coverage. For surface water, these data are increasingly being coupled to global hydrological models. The upcoming NASA/CNES Surface Water Ocean Topography (SWOT) science mission will be used, in part, to help calibrate and improve such global models. Also, the GPM mission, and its planned follow-ons, are to establish the improvements in global precipitation data that will allow increasingly accurate model predictions, including flood predictions for developing nations (Webster 2013). An overarching challenge is to harness these new global "disruptive technologies" for the local public good. These new capabilities are novel but also overlap with existing governmental functions such as flood alerts and warnings.

Remotely sensed images can deliver key products for early warning, for the planning of life-saving activities and for impact assessment in the phases immediately following a hydrometeorological disaster. The DFO is both providing near real-time products and collecting trusted information from other services involved in the Global Flood Partnership. Recent system developments have taken the DFO into the era of interoperability and are now offering a whole suite of different data products also from other organizations, including many EO flood products but also forecasts and flood hazard simulations, with the objective to help mitigate and respond to flood disasters at the global level. Future developments may include complementing EO and model layers with social media streams to help verify areas affected or pinpoint target regions for satellite image acquisitions. Of course, this functionality will require the highest level of interoperability

since all of it needs to integrate seamlessly with end-user operation systems and mapping platforms and ideally also be accessible on any device. In this context, strengthening public-private partnerships would allow access to high-end capabilities leveraging advanced data interoperability standards and service protocols developed by the geospatial industry sector. The ability of communities to understand and use this information is also an important aspect.

Matching capabilities and needs is also a key aspect for SEM mechanisms. The IWG-SEM role in the definition of both mapping guidelines and standard formats/products could foster better agreement between maps produced by different organizations involved in the mechanism. Solving restrictive data licensing could further increase data availability in the aftermath of disasters.

The role of satellites is not limited to the emergency phase. Activities in the recovery phase, especially in areas where the agricultural sector is dominant, can take advantage of the possibility of performing reliable analysis with wide spatial coverage and frequent updates from satellites. Short-term damage assessment can take advantage of the information produced by SEM mechanisms without necessarily planning further satellite acquisitions whereas a similar analysis performed with in-situ observation would require a more massive resource-intensive effort.

6. REFERENCES

Bai, Z.G., Dent, D.L., Olsson, L., Schaepman, M.E. (2008). Global assessment of land degradation and improvement 1: identification by remote sensing. Report 2008/01. https://www.isric.org/sites/default/files/isric_report_2008_01.pdf Accessed 30 October 2020.

Brakenridge, R., & Anderson, E. (2006). Modis-based flood detection, mapping and measurement: the potential for operational hydrological applications. In J. Marsalek, G. Stancalie, G. Balint (Eds.), *Transboundary Floods: Reducing Risks Through Flood Management* (pp. 1-12). Dordrecht: Springer Netherlands.

Brakenridge, G.R., Cohen, S., Kettner, A.J., De Groeve, T., Nghiem, S. V, Syvitski, J.P.M., et al. (2012). Calibration of satellite measurements of river discharge using a global hydrology model. *Journal of Hydrology, 475*, 123–136. https://doi.org/10.1016/j.jhydrol.2012.09.035

Copernicus EMS (2019a). Copernicus EMS monitor major Tropycal Cyclone in Mozambique. https://emergency.copernicus.eu/mapping/ems/copernicus-ems-monitors-major-tropical-cyclone-mozambique. Accessed 30 October 2020.

Copernicus EMS (2019b). EU provides further support for Mozambique following Cyclone Idai. https://emergency.copernicus.eu/mapping/ems/eu-provides-further-support-mozambique-following-cyclone-idai. Accessed 30 October 2020.

Copernicus EMS (2019c). Copernicus EMS monitors impact of Cyclone Kenneth in Mozambique and Comoros. https://emergency.copernicus.eu/mapping/ems/copernicus-ems-monitors-impact-cyclone-kenneth-mozambique-and-comoros. Accessed 30 October 2020.

Copernicus EMS (2020). Service overview. https://emergency.copernicus.eu/mapping/ems/service-overview. Accessed 30 October 2020.

de Bruijn, J.A., de Moel, H., Jongman, B., de Ruiter, M.C., Wagemaker, J., Aerts, J.C.J.H. (2019). A global database of historic and real-time flood events based on social media. *Scientific data, 6*, 311. https://doi.org/10.1038/s41597-019-0326-9

Denis, G., de Boissezon, H., Hosford, S., Pasco, X., Montfort, B., Ranera, F. (2016). The evolution of Earth Observation satellites in Europe and its impact on the performance of emergency response services. *Acta Astronautica*, *127*, 619-633. https://doi.org/10.1016/j.actaastro.2016.06.012

DFO (2020a). Dartmouth Flood Observatory. http://floodobservatory.colorado.edu. Accessed 30 October 2020.

DFO (2020b). River and Reservoir Watch. http://floodobservatory.colorado.edu/DischargeAccess.html. Accessed 30 October 2020.

DFO (2020c). DFO Web Map Service. http://floodobservatory.colorado.edu/WebMapServerDataLinks.html. Accessed 30 October 2020.

Dottori, F., Salamon, P., Bianchi, A., Alfieri, L., Hirpa, F.A., Feyen, L. (2016). Development and evaluation of a framework for global flood hazard mapping. *Advances in Water Resources, 94*, 87–102. https://doi.org/10.1016/j.advwatres.2016.05.002

Eklundh, L., Jönsson, P. (2017). Timesat 3.3 Software Manual. Lund and Malmö University, Sweden. http://web.nateko.lu.se/timesat/docs/TIMESAT33_SoftwareManual.pdf. Accessed 17 October 2020.

ERCC – DG ECHO (2019a). Tropical Cyclone Idai impact overview. https://erccportal.jrc.ec.europa.eu/getdailymap/docId/2860. Accessed 30 October 2020.

ERCC – DG ECHO (2019b). TC Idai: EU response. https://erccportal.jrc.ec.europa.eu/getdailymap/docId/2869. Accessed 30 October 2020.

ERDS (2020). Extreme Rainfall Detection System. http://erds.ithacaweb.org. Accessed 30 October 2020.

Fekete, B.M., Vörösmarty, C.J., Grabs, W. (2002). High-resolution fields of global runoff combining observed river discharge and simulated water balances. *Global Biogeochemical Cycles*, *16*, 10–15. https://doi.org/10.1029/1999GB001254

Fensholt, R., Sandholt, I., Stisen, S. (2006). Evaluating MODIS, MERIS, and vegetation indices using in situ measurements in a semiarid environment. *IEEE Transactions on Geoscience and Remote Sensing, 44*(7), 1774–1786. https://doi.org/10.1109/TGRS.2006.875940

Hmimina, G., Dufrene, E., Pontailler, J.Y., Delpierre, N., Aubinet, M., Caquet, B., et al. (2013). Evaluation of the potential of MODIS satellite data to predict vegetation phenology in different biomes: an investigation using ground-based NDVI measurements. *Remote Sensing of Environment, 132*, 145–158. https://doi.org/10.1016/j.rse.2013.01.010

Huffman, G.J., Bolvin, D.T., Nelkin, E.J., Tan, J. (2019). Integrated Multi-satellitE Retrievals for GPM (IMERG) Technical Documentation. https://pmm.nasa.gov/sites/default/files/document_files/IMERG_doc_190909.pdf. Accessed 30 October 2020.

IWG-SEM (2014). Technical specification of GeoRSS, Version 1. http://www.un-spider.org/sites/default/files/20141126_GeoRSS_technical_specifications.pdf. Accessed 30 October 2020.

IWG-SEM (2015). Emergency Mapping Guidelines, Working Paper Version 1.0. http://www.un-spider.org/sites/default/files/IWG_SEM_EmergencyMappingGuidelines_v1_Final.pdf. Accessed 30 October 2020.

Jongman, B., Wagemaker, J., Revilla Romero, B., Coughlan De Perez, E. (2015). Early flood detection for rapid humanitarian response: harnessing near real-time satellite and Twitter signals. *ISPRS International Journal of Geo-Information*, *4*(4), 2246-2266. https://doi.org/10.3390/ijgi4042246

Mazzoglio, P., Laio, F., Balbo, S., Boccardo, P., Disabato, F. (2019). Improving an Extreme Rainfall Detection System with GPM IMERG data. *Remote Sensing*, *11*(6), 677. https://doi.org/10.3390/rs11060677

NASA (2020). About SERVIR. https://www.nasa.gov/mission_pages/servir/overview.html. Accessed 30 October 2020.

Nguyen, P., Shearer, E.J., Tran, H., Ombadi, M., Hayatbini, N., Palacios, T., et al. (2019). The CHRS data portal, an easily accessible public repository for PERSIANN global satellite precipitation data. *Scientific Data*, *6*, 180296. https://doi.org/10.1038/sdata.2018.296

Nguyen, P., Shearer, E.J., Ombadi, M., Gorooh, V.A., Hsu, K., Sorooshian, S., et al. (2020). PERSIANN Dynamic Infrared-Rain rate model (PDIR) for high-resolution, real-time satellite precipitation estimation. *Bulletin of the American Meteorological Society*, *101*, E286-E302. https://doi.org/10.1175/BAMS-D-19-0118.1

Pettorelli, N., Vik, J.O., Mysterud, A., Gaillard, J.M., Tucker, C.J., Stenseth, N.C. (2005). Using the satellite-derived NDVI to assess ecological responses to environmental change. *Trends in ecology & evolution*, *20*(9), 503–510. https://doi.org/10.1016/j.tree.2005.05.011

Reed, B.C., Brown, J.F., VanderZee, D., Loveland, T.R., Merchant, J.W., Ohlen, D.O. (1994). Measuring phenological variability from satellite imagery. *Journal of Vegetation Science*, *5*, 703–714. https://doi.org/10.2307/3235884

Running, S.W., Nemani, R.R., Heinsch, F.A., Zhao, M., Reeves, M., Hashimoto, H. (2004). A continuous satellite-derived measure of global terrestrial primary production. *BioScience*, *54*(6), 547–560. https://doi.org/10.1641/0006-3568(2004)054[0547:ACSMOG]2.0.CO;2

Schumann, G.J.P., & Domeneghetti, A. (2016). Exploiting the proliferation of current and future satellite observations of rivers. *Hydrological Processes*, *30*, 2891-2896. https://doi.org/10.1002/hyp.10825

Schumann, G.J.P., Brakenridge, G.R., Kettner, A.J., Kashif, R., Niebuhr, E. (2018). Assisting flood disaster response with earth observation data and products: a critical assessment. *Remote Sensing*, *10*(8), 1230. https://doi.org/10.3390/rs10081230

Schumann, G.J.P. (2019). The need for scientific rigour and accountability in flood mapping to better support disaster response. *Hydrological Processes*, *33*, 3138-3142. https://doi.org/10.1002/hyp.13547

Sentinel Asia (2020). About Sentinel Asia. https://sentinel-asia.org/aboutsa/AboutSA.html. Accessed 30 October 2020.

The International Charter Space and Major Disasters (2019a). Charter geobrowser tool, activation 598. https://cgt.disasterscharter.org/en/598. Accessed 30 October 2020.

The International Charter Space and Major Disasters (2019b). Charter geobrowser tool, activation 606. https://cgt.disasterscharter.org/en/606. Accessed 30 October 2020.

The International Charter Space and Major Disasters (2019c). Cyclone Idai in Mozambique. https://disasterscharter.org/web/guest/activations/-/article/cyclone-in-mozambique-activation-598-. Accessed 30 October 2020.

The International Charter Space and Major Disasters (2019d). Cyclone Idai in Zimbabwe. https://disasterscharter.org/web/guest/activations/-/article/cyclone-in-zimbabwe-activation-599-. Accessed 30 October 2020.

The International Charter Space and Major Disasters (2020). About the Charter. https://disasterscharter.org/web/guest/about-the-charter. Accessed 30 October 2020.

Tucker, C.J. (1979). Red and photographic infrared linear combinations for monitoring vegetation. *Remote Sensing of Environment*, *8*(2), 127–150. https://doi.org/10.1016/0034-4257(79)90013-0

UN General Assembly (2015). Transforming our world: the 2030 Agenda for Sustainable Development, A/RES/70/1. https://www.refworld.org/docid/57b6e3e44.html. Accessed 30 October 2020.

UN-SPIDER (2020). UN-SPIDER Knowledge Portal. http://www.un-spider.org/space-application/emergency-mechanisms. Accessed 30 October 2020.

UNOSAT (2020). UNOSAT Rapid mapping service. https://www.unitar.org/maps/unosat-rapid-mapping-service. Accessed 30 October 2020.

Voigt, S., Giulio Tonolo, F., Lyons, J., Kučera, J., Jones, B., Schneiderhan, T., et al. (2016). Global trends in satellite-based emergency mapping. *Science*, *353*(6296), 247-252. https://doi.org/10.1126/science.aad8728

Webster, P.J. (2013). Improve weather forecasts for the developing world. *Nature*, *493*, 17-19. https://doi.org/10.1038/493017a

WFP (2019). Mozambique access constraints as of 16 March 2019. https://reliefweb.int/sites/reliefweb.int/files/resources/moz_op_accessconstraints_a3p_20190316.pdf. Accessed 30 October 2020.

World Bank 2020. Cereal yield (kg per hectare) – Mozambique. https://data.worldbank.org/indicator/AG.YLD.CREL.KG?locations=MZ. Accessed 30 October 2020.

Wu, H., Adler, R.F., Tian, Y., Huffman, G.J., Li, H., Wang, J. (2014). Real-time global flood estimation using satellite-based precipitation and a coupled land surface and routing model. *Water Resources Research*, *50*, 2693-2717. http://doi.org/10.1002/2013WR014710